Electronic Supplementary Material (ESI) for Analyst.
This journal is © The Royal Society of Chemistry 2019

Supporting Information

Rational design of a novel turn-on fluorescent probe for detecting hydrazine with barbituric acid as recognition group and bioimaging

Junli Du[a,b], Xiaolu Li[a,b], Songsong Ruan[a,b], Yingchun Li[a], Fan Ren[a,b], Yanjun Cao[a], Xiaoqing Wang[c], Yongmin Zhang[a,b,d], Shaoping Wu[a,b*], Jianli Li[c]

[a] School of Pharmacy; Key Laboratory of Resource Biology and Biotechnology in Western China (Northwest University), Ministry of Education; Biomedicine Key Laboratory of Shaanxi Province, Northwest University, Xi'an 710069, China

[b] Joint International Laboratory of Glycobiology and Medicinal Chemistry, Northwest University, Xi'an, Shaanxi 710069, China

[c] Key Laboratory of Synthetic and Natural Functional Molecule Chemistry of Ministry of Education, College of Chemistry & Materials Science, Northwest University, Xi'an, Shaanxi 710127, P. R. China

[d] Sorbonne Université, Institut Parisien de Chimie Moléculaire, CNRS UMR 8232, 4 place Jussieu, 75005 Paris, France

* Tel.: +86 029 88304569; Fax: +86 029 88304569. E-mail: wushaoping@nwu.edu.cn

CONTENTS

1. Recent progress in the development of fluorescent probes for the detection of $N_2H_4 \cdot H_2O$

Ref	Probe structures	λ_{ex}	λ_{em}	LOD(M)	Sensing pH ranges	Response Time	Biological imaging application
[1]	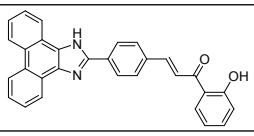	415 nm	458 nm, 562 nm	7.4×10^{-8} M	7-10	30 min	HeLa cells
[2]	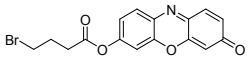	560 nm	584 nm	2×10^{-6} M	7-10	60 min	Chinese hamster ovary (CHO) cells
[3]	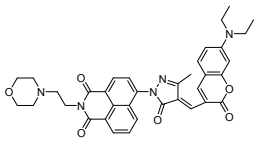	440 nm	517 nm	1.4×10^{-7} M	4-10	8 min	HeLa cells
[4]	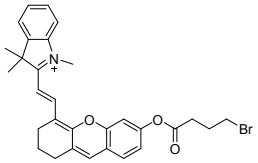	685 nm	715 nm	1.6×10^{-7} M 5.09 ppb	6-8	30 min	HeLa cells and mice
[5]	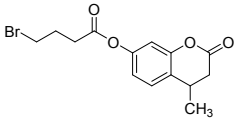	365 nm	450 nm	7×10^{-8} M	7-9	30 min	HeLa cells
[6]	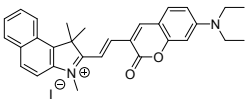	450 nm	510 nm, 660 nm	5.6×10^{-7} M	4-10	24 h	-
[7]	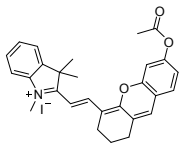	675 nm	706 nm	1.7×10^{-7} M	4-10	10 min	HeLa cells and Kunming mouse
[8]	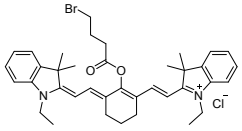	580 nm, 780 nm	627 nm, 814 nm	1.2×10^{-8} M 0.38 ppb	5-8	17 min	HeLa cells and mice
[9]	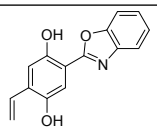	390 nm	560 nm	8.42×10^{-8} M (2.7 ppb)	4-10	7 min	HeLa cells
[10]	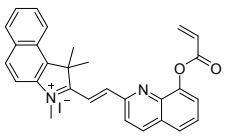	405 nm	590 nm	2.1×10^{-6} M	5-10	4 min	$HepG_2$ cells
[11]	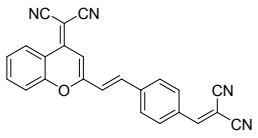	460 nm	532 nm, 660 nm	7.71×10^{-9} M	3-10	60 min	MCF-7 cells

Our work	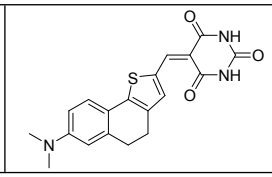	380 nm	527 nm	5×10^{-8} M	3-12	10 min	SH-SY5Y cells

2. Calculation of the detection limit of probe DPT

$$\mathrm{LOD}=\frac{3\sigma}{\mathrm{k}}$$

Where σ is the standard deviation of the blank measurement, k is the slope between the fluorescence intensity and concentration $\mathbf{N_2H_4{\cdot}H_2O}$ (0~26 μM). The fluorescence intensity of **DPT** was measured by eleven times and the standard deviation of the blank measurement was achieved. The calculated LOD of probe **DPT** are showed in **Table S1.**

Table S1. Calculated detection limit for probe **DPT.**

Probe	DPT
LOD/nM	50

3. Calculation of fluorescence quantum yield about probe DPT

The quantum yield (***Φ***) of **DPT** denotes the fluorescence quantum yield. It was measured at room temperature referenced to fluorescein in aqueous solution of 0.1 M sodium hydroxide, which has a quantum yield of 0.92. We calculated the fluorescence quantum yield of **DPT** in different organic solvents. The results were shown in **Table S2.**

Table S2. Calculated the fluorescence quantum yields for **DPT** in different organic solvents.

Solvent	MeOH	EtOH	ACN	DMK	DMSO	DMF	TCM	DCM	EtOAc	H_2O	THF
Φ_f	0.12	0.26	0.30	0.52	0.41	0.38	0.19	0.56	0.54	0.07	0.49

$\mathbf{\Phi_S}$ was quantum yield of fluorescein; $\mathbf{A_X}$ and $\mathbf{A_S}$ indicated the absorption intensity of the sample and the standard at the excitation wavelength, respectively; $\mathbf{F_X}$ and $\mathbf{F_S}$ for the sample and the standard fluorescence integral area; **n** was refractive index of the solvent; Subscript **s** and **x** was the standard and unknown samples, respectively.

$$\Phi_{\mathrm{F(X)}} = \Phi_{F(S)} \times \left(\frac{A_S \times F_X}{A_X \times F_S} \right) \left(\frac{n_X}{n_S} \right)^2$$

4. Synthesis of compound **1** and **2**

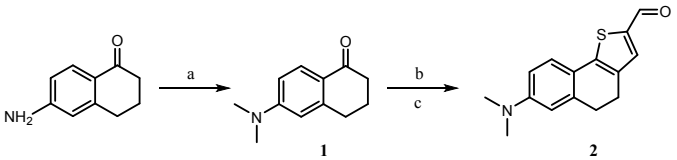

Scheme S1. Reagents and conditions: (a) CH_3I, K_2CO_3, DMF, 50 ℃, 24 h, 48.2%; (b) $POCl_3$, DMF, 90 ℃, 5 h; (c) $Na_2S·9H_2O$, C_2H_3ClO, DMF, 60 ℃, 5 h, 52.1% for two steps.

*1) Synthesis of compound 6-(dimethylamino)-3,4-dihydronaphthalen-1(2H)-one (**1**)*

CH_3I (0.42 mL, 6.82 mmol, 5.5 equiv.) was added to a mixture of 6-amino-3,4-dihydronaphthalen-1(2H)-one (200 mg, 1.24 mmol, 1.0 equiv.) and K_2CO_3 (377 mg, 2.73 mmol, 2.2 equiv.) in DMF (18 mL) and the mixture was protected from light and stirred for 24 h at 50 °C. After cooling to room temperature, water (10 mL) was added and the solution was extracted with EtOAc and washed with water and brine. The organic layer was combined and dried with anhydrous Na_2SO_4 and evaporated under reduced pressure. The obtained residue was dried and purified by column chromatography on silica gel (petroleum ether/EtOAc, 2:1 v/v) to give compound **1** as a light ginger yellow solid (yield: 48.2 %, R_f = 0.60).

*2) Synthesis of compound 7-(dimethylamino)-4,5-dihydronaphtho[1,2-b] thiophene-2-carbaldehyde (**2**)*

$POCl_3$ (88.5 μL, 0.95 mmol, 1.3 equiv.) was added dropwise to a flask under nitrogen containing DMF (4 mL) with stirring at 0 ℃ over 30 min. Compound **1** (138 mg, 0.73 mmol, 1.0 equiv.) in DMF was added slowly with stirring and the mixture was heated for 5 h at 90 ℃. Then the mixture was poured to ice water and the resulting precipitate was filtered off and washed with cold water to afford the 1-chloro-6-(dimethylamino)-3,4-dihydronaphthalene-2-carbaldehyde as yellow solid, which was utilized in the next reaction without further purification.

To a solution of $Na_2S·9H_2O$ (72 mg, 0.30 mmol, 1.1 equiv.) and DMF (5 mL) was added 1-chloro-6-(dimethylamino)-3,4-dihydronaphthalene-2-carbaldehyde (63.4 mmol, 0.27 mmol, 1.0 equiv.). The mixture was stirred at 60 ℃ during 2 h.

Chloroacetaldehyde (50 μL, 0.30 mmol, 1.1 equiv.) was added rapidly and the reaction was stirred during 3 h at 60 ℃. K_2CO_3 (41.5 mg, 0.30 mmol, 1.1 equiv.) was dissolved in water (1.0 mL) and added to the reaction. The mixture was stirred during 10 min at 60 ℃, cooled at room temperature and quenched in water. The resulting mixture was extracted with ethyl acetate. The organic layer was combined and dried with anhydrous Na_2SO_4 and evaporated under reduced pressure. The obtained residue was dried and purified by column chromatography on silica gel (petroleum ether/EtOAc, 3:1 v/v) to give compound **2** as a brown solid (yield: 52.1% in two steps, R_f = 0.61).

5. Optical properties of DPT in different organic solvents

The optical properties of **DPT** in different organic solvents included the maximum absorption wavelength (λ_{abs})、Molar absorption coefficient (ε_{max})、Emission wavelength、Stokes shift. The calculation results are shown in **Table S3.** We could get that there was a large Stokes shift for **DPT**.

Table S3. Optical properties of **DPT** in different organic solvents.

Solvent	λ_{abs}/nm	ε_{max}/$M^{-1}\cdot cm^{-1}$	λ_{em}/nm[a]	$\Phi_{F(X)}$	Stokes shift	
					nm	cm^{-1}
MeOH	558	27867	547	0.12	167	8034
EtOH	558	31333	507	0.26	127	6573
ACN	549	16667	500	0.30	120	6296
DMK	543	28800	495	0.52	115	6114
DMSO	554	43867	495	0.41	115	6093
DMF	549	47867	494	0.38	114	6052
TCM	572	42267	493	0.19	113	6032
DCM	566	36400	491	0.56	111	5949
EtOAc	536	35067	490	0.54	110	5887
H_2O	547	6133	490	0.07	110	5887
THF	538	50000	484	0.49	104	5633

a: λ_{ex} = 380 nm.

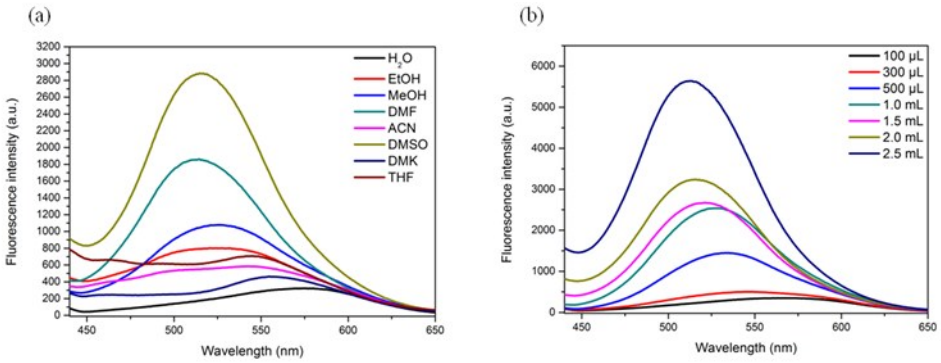

Fig. S1. (a) Fluorescence spectra of **DPT** (10 μM) in different organic solvents with $N_2H_4 \cdot H_2O$ (20 μM); (b) Fluorescence spectra of **DPT** (10 μM) in various volumes of DMSO with $N_2H_4 \cdot H_2O$ (20 μM). λ_{ex} = 380 nm; slits: (5 nm/5 nm).

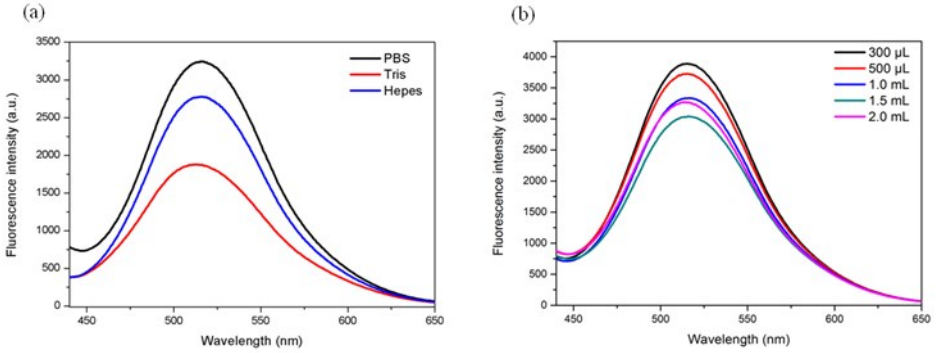

Fig. S2. (a) Fluorescence spectra of **DPT** (10 μM) in different buffers with $N_2H_4 \cdot H_2O$ (20 μM); (b) Fluorescence spectra of **DPT** (10 μM) in various volumes of PBS buffer with $N_2H_4 \cdot H_2O$ (20 μM). λ_{ex} = 380 nm; slits: (5 nm/5 nm).

6. Fluorescence spectra of probe DPT reaction with $N_2H_4 \cdot H_2O$

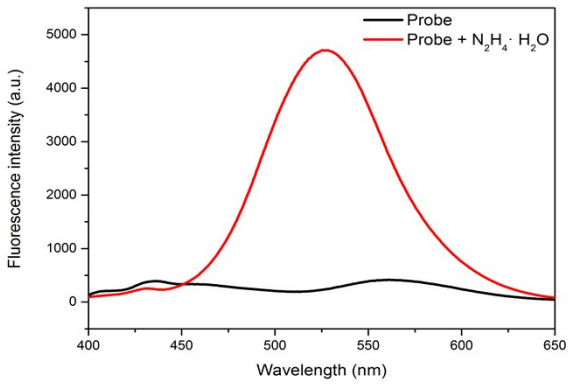

Fig. S3. Fluorescence spectra of probe **DPT** reaction with $N_2H_4 \cdot H_2O$.

7. Characterization data of the intermediate and probe DPT

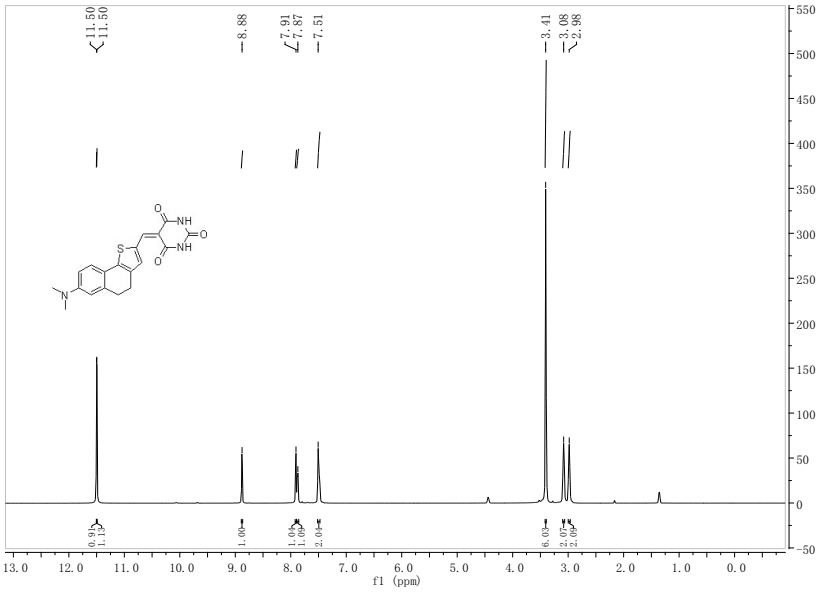

Fig. S4. ^{1}H-NMR spectrum of probe **DPT** in TFA-d_1.

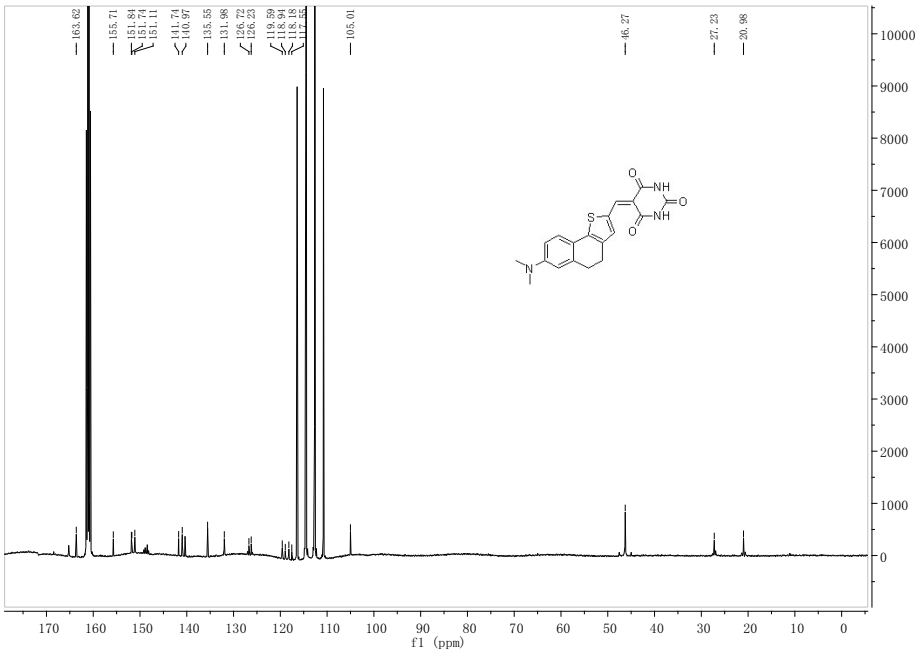

Fig. S5. ^{13}C-NMR spectrum of probe **DPT** in TFA-d_1.

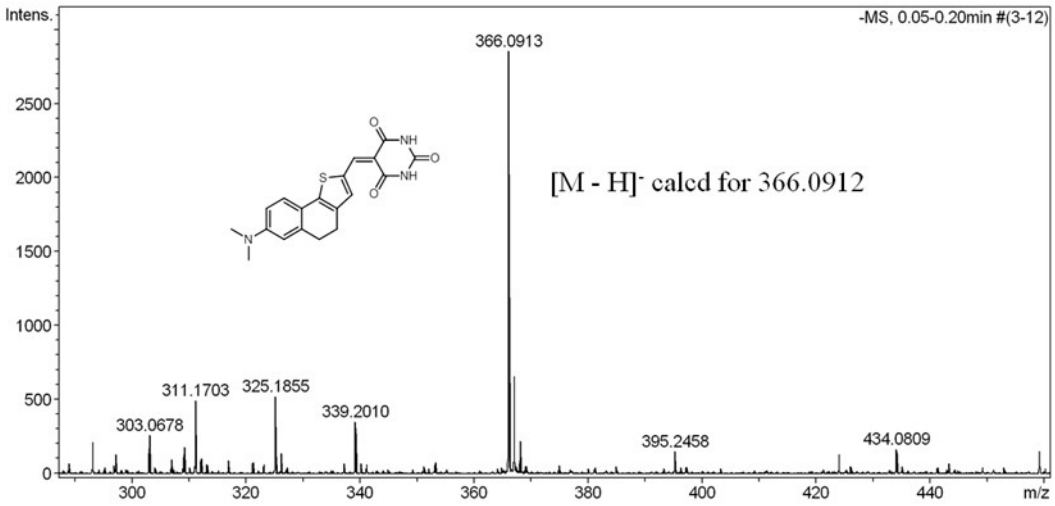

Fig. S6. HRMS of probe **DPT**.

8. Proposed reaction mechanism of detecting $N_2H_4 \cdot H_2O$

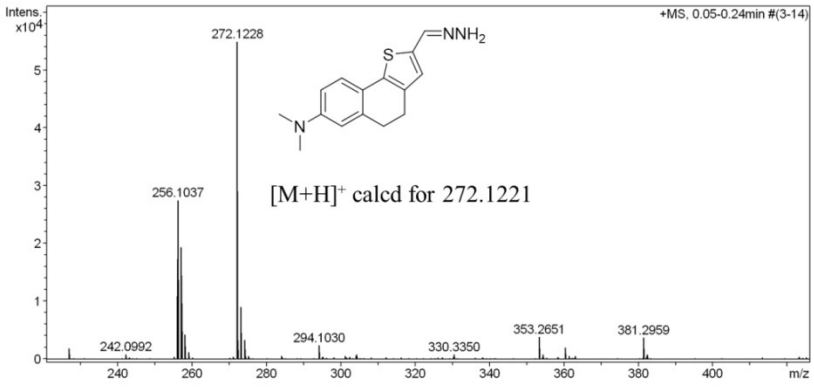

Fig. S7. Proposed reaction mechanism of detecting $N_2H_4 \cdot H_2O$.

9. DFT optimized structures of probe DPT and DPT-N_2H_4

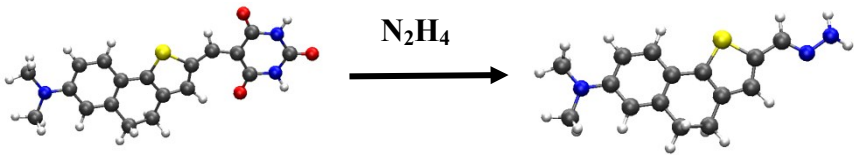

DPT **DPT-N_2H_4**

Fig. S8. Density functional theory optimized structures of **DPT** and compound **DPT-N_2H_4**.

10. Cytotoxicity experiment of probe DPT

The cell viability (%) was assessed using the following equation:

Cell viability (%) = T/C × 100%, where T is the OD_{450} value of experience group and C is the control group of OD_{450} (***optical density***) value.

OD_{450} value of each repeated wells are given as mean ± standard deviation (SD)

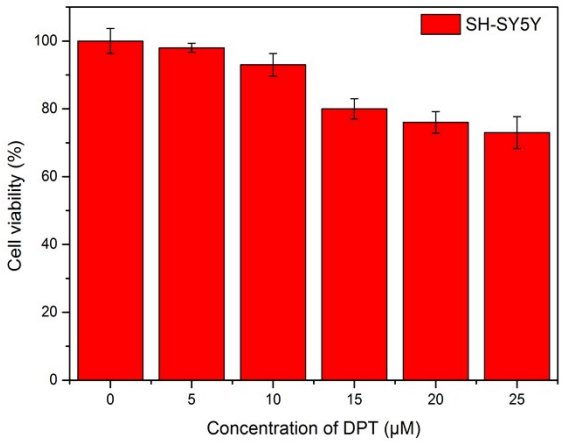

Fig. S9. Cytotoxicity assays of probe **DPT** at different concentrations (0 μM, 5 μM, 10 μM, 15 μM, 20 μM, 25 μM) for SH-SY5Y neuroblastoma cells.

References

[1] H. Xu, B. Gu, Y. Q. Li, Z. Huang, W. Su, X. L. Duan, P. Yin, H. Li, S. Yao, *Talanta*, 2018, 180, 199-205.

[2] Y. Qian, J. Lin, L. J. Han, L. Lin, H. L. Zhu, *Biosens Bioelectron*, 2014, 58, 282-286.

[3] B. J. Shi, Y. Y. He, P. P. Zhang, Y. L. Wang, M. M. Yu, H. Y. Zhang, L. H. Wei, Z. X. Li, *Dyes Pigm.*, 2017, 147, 152-159.

[4] Z. L. Lu, X. M. Shi, Y. F. Ma, W. L. Fan, Y. A. Lu, Z. Zhou, C. H. Fan, *Sens. Actuators, B*, 2018, 258, 42-49.

[5] S. Chen, P. Hou, J. Wang, L. Liu, Q. Zhang, *Spectrochim. Acta, Part A*, 2017, 173, 170-174.

[6] Y. Y. He, Z. X. Li, B. J. Shi, Z. An, M. M. Yu, L. H. Wei, Z. H. Ni, *RSC Adv.*, 2017, 7, 25634-25639.

[7] J. J. Zhang, L. L. Ning, J. T. Liu, J. X. Wang, B. F. Yu, X. Y. Liu, X. J. Yao, Z. P. Zhang, H. X. Hai, *Anal. Chem.*, 2015, 87, 9101-9107.

[8] Z. L. Lu, W. L. Fan, X. M. Shi, Y. Y. Lu, C. H. Fan, *Anal. Chem.*, 2017, 89, 9918-9925.

[9] L. L. Xiao, J. Tu, S. G. Sun, Z. C. Pei, Y. X. Pei, Y. Pang, Y. Q. Xu, *RSC Adv.*, 2014, 4, 41807-41811.

[10] Y. A. Ban, R. H. Wang, Y. Li, Z. An, M. M. Yu, C. J. Fang, L. H. Wei, Z. X. Li, *New J. Chem.*, 2018, 42, 2030-2035.

[11] X. P. Yang, Y. X. Liu, Y. Y. Wu, X. L. Ren, D. Zhang, Y. Ye, *Sens. Actuators, B*, 2017, 253, 488-494.